XPS Valence Band Studies of LaNi$_{5-x}$M$_x$ (M = Al, Co; $x = 0, 1$) Alloy Thin Films

J. Skoryna^{a,*}, A. Marczyńska^a, S. Pacanowski^b, A. Szajek^a and L. Smardz^a

^{a}Institute of Molecular Physics, Polish Academy of Sciences, M. Smoluchowskiego 17, 60-179 Poznań, Poland

^{b}Faculty of Technical Physics, Poznań University of Technology, Piotrowo 3, 60-965 Poznań, Poland

LaNi$_{5-x}$M$_x$ (M = Al, Co) alloy thin films were prepared onto oxidised Si(100) substrates in the temperature range of 285–700 K using UHV magnetron co-sputtering. The surface chemical composition and valence bands of all the alloy thin films were measured *in situ*, immediately after deposition, transferring the samples to an UHV analysis chamber equipped with X-ray photoelectron spectroscopy. Results showed that the shape of the valence bands measured for the polycrystalline samples is practically the same compared to those obtained theoretically from *ab initio* band structure calculations. On the other hand, the X-ray photoelectron spectroscopy valence bands of the nanocrystalline thin films (especially LaNi$_4$Co) are considerably broader compared to those measured for the polycrystalline samples. This is probably due to a strong deformation of the nanocrystals. Therefore, the different microstructure observed in polycrystalline and nanocrystalline alloy thin films leads to significant modifications of their electronic structure.

1. Introduction

Reversible charging and discharging at moderate temperatures together with high volumetric and gravimetric densities is required for the utilization of hydrogen as an energy carrier. The intermetallic compound LaNi$_5$ is well known for its ability to store hydrogen reversibly at pressures and temperatures of interest for applications close to ambient conditions [1]. Therefore, it serves as a reference compound to understand the physical and chemical phenomena of the hydrogenation process.

Several semi-empirical models [2, 3] have been proposed for the heat of formation and heat of solution of metal hydrides and attempts have been made for justifying the maximum hydrogen absorption capacity of the metallic matrices. These models showed that the energy of the metal–hydrogen interaction depends both on geometric and electronic factors. In order to optimise the choice of the nanocomposites for a selected application, a better understanding of the role of each alloy constituent on the electronic properties of the material is crucial. In a recent paper [4] we showed that the valence bands of bulk nanocrystalline and nanocomposite LaNi$_5$ based materials were broadened compared to those measured for polycrystalline samples with the similar average chemical compositions. Furthermore, practically the all mechanically alloyed nanomaterials showed significantly greater discharge capacity [4]. On the other hand, in Pd clusters hydrogen solubility increases in alpha-phase, whereas the minimum beta-phase solubility is reduced, which results in the lowering of miscibility gap compared to that measured for bulk palladium [5]. In this contribution, we study experimentally and theoretically the electronic properties of polycrystalline and nanocrystalline LaNi$_{5-x}$M$_x$ (M = Al, Co; $x = 0, 1$) alloy thin films using X-ray photoelectron spectroscopy (XPS) and *ab initio* band structure calculations, respectively.

2. Experimental procedure

LaNi$_{5-x}$M$_x$ (M = Al, Co; $x = 0, 1$) alloy thin films were prepared onto oxidised Si(100) substrates in the temperature range of 285–700 K using computer-controlled ultra high vacuum (UHV) magnetron co-sputtering. Ni(Co, Al) and La targets were sputtered using DC and RF modes, respectively. The total thickness of the samples was about 1000 nm. The base pressure before the deposition process was lower than 5×10^{-10} mbar. As a substrate we have used Si(100) wafers with an oxidised surface to prevent a silicide formation. Therefore we have applied a special heat treatment in UHV before deposition in order to obtain an epitaxial SiO$_2$ surface layer [6]. The distance between sputtering targets and substrate was about 220 mm.

The chemical composition and the cleanness of all layers was checked *in situ*, immediately after deposition, transferring the samples to an UHV analysis chamber equipped with XPS [4]. The electronic properties of the prepared samples were studied *in situ* using XPS. The structure of the samples has been studied by X-ray diffraction (XRD). Their bulk chemical compositions were measured using X-ray fluorescence (XRF) method.

The band structures were calculated using the *ab initio* full-potential local-orbital method in the coherent potential approximation (FPLO-CPA) [7, 8]. The theoretical photoemission spectra were obtained from the calculated densities of electronic states convoluted by Gaussian with a half-width (δ) equal to 0.6 eV and scaled using the proper photoelectronic cross-sections for partial states [9].

_____

*corresponding author; e-mail: jskoryna@ifmpan.poznan.pl

3. Results and discussion

Results on XRF measurements revealed the assumed bulk chemical composition of the prepared alloy thin films. Structural studies showed that the samples deposited at 285 K are nanocrystalline with average grain size $D \approx 15-20$ nm. Thin films deposited at about 700 K are polycrystalline with $D \approx 150-200$ nm.
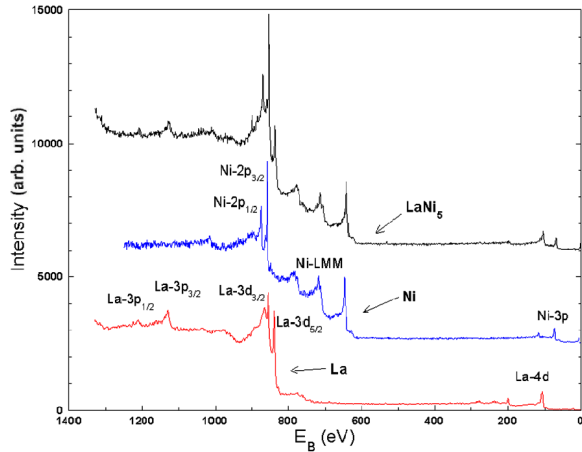

Fig. 1. XPS (Al K_α) spectrum of the freshly prepared polycrystalline LaNi$_5$ alloy thin film (top curve). For a comparison we also show the XPS spectra measured for *in situ* prepared polycrystalline Ni and La thin films. The total thickness of the samples was about 1000 nm.

In Fig. 1 we show XPS core-level spectra of the freshly deposited polycrystalline La, Ni, and LaNi$_5$ thin films. The total thickness of the prepared thin film samples was about 1000 nm. Due to well known high reactivity of lanthanum with oxygen we have prepared the nanocrystalline alloy thin films after an additional heating of the sample holder and new substrate at 700 K for 3 h and cooling to 285 K. Results showed that after such an outgassing procedure, it is possible to prepare oxygen and carbon free La and LaNi$_5$ surface. The corresponding XPS spectra are shown in Fig. 1. The oxygen and other surface impurities are practically absent on such prepared La-based alloy thin films immediately after deposition. As can be seen in Fig. 1, practically no XPS signal from potential contamination atoms like O 1s and C 1s is observed. On the other hand, we have observed oxygen atoms (below 1 at.%) already adsorbed on La and LaNi$_5$ surface 1 h and 3 h after preparation, respectively. Note that the sample was kept in the analysis chamber in vacuum of 6×10^{-11} mbar.

In Fig. 2 we show the XPS valence bands for polycrystalline LaNi$_5$ thin film. The shape and position of the valence band measured for the polycrystalline LaNi$_5$ alloy thin film (bold solid line, top part in Fig. 2) are practically the same compared to those calculated from the *ab initio* method. For comparison we also show the XPS spectra measured for *in situ* prepared polycrystalline 1000 nm Ni and 1000 nm La thin films (see top part in Fig. 2). The major contribution to the total XPS signal originated from the Ni atoms is in the 3g positions
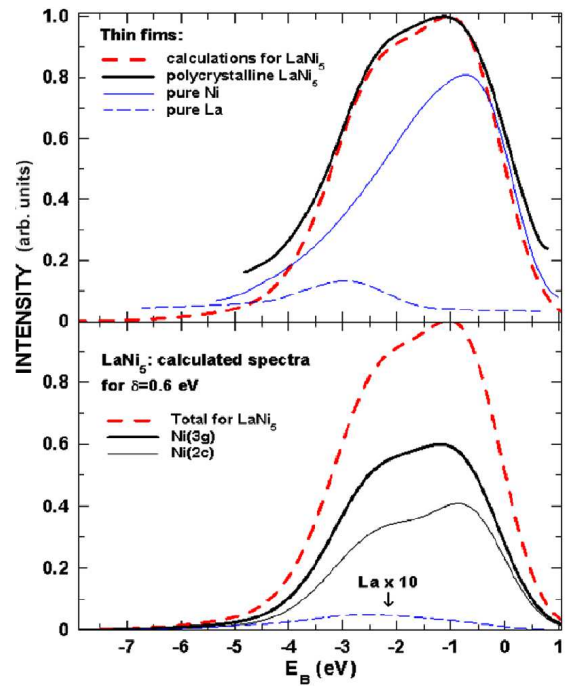

Fig. 2. Experimental (bold solid line, top part) and theoretical (broken line, top part) XPS valence band spectra for *in-situ* prepared polycrystalline LaNi$_5$ alloy thin films. For a comparison we also show the XPS valence band spectra measured for *in-situ* prepared polycrystalline 1000 nm Ni and 1000 nm La thin films (top part). Local contribution of Ni and La atoms to the total theoretical XPS are shown in bottom part.

(see bottom part in Fig. 2). On the other hand, the influence of the La atoms on the XPS valence band is rather small.

The experimental valence bands measured for poly- and nanocrystalline LaNi$_4$Co thin films are shown in Fig. 3 (top part). We have observed a small (0.1 eV) shift to the lower binding energy and broadening of the valence band measured for the nanocrystalline sample compared to that determined for the polycrystalline thin film. The above behaviour could be explained as strong deformation of the nanocrystals [4]. For such nanocrystalline samples the interior of the nanocrystal is constrained and the distances between atoms located at the grain boundaries are expanded [10]. Very similar valence band broadening we have observed earlier for the LaNi$_5$-type bulk nanocrystalline alloys [4]. The maximum of the theoretical XPS valence band is slighty shifted to the Fermi level compared to those determined experimentally. According to the *ab initio* calculations the main contribution to the total XPS signal originated from Ni atoms is in 2c and 3g positions (see bottom part in Fig. 3).

Figure 4 (top part) shows the XPS valence band spectra measured for the nano- (bold solid line) and polycrystalline (thin solid line) LaNi$_4$Al thin films. We have observed a small broadening of the binding energy of the valence band measured for the nanocrystalline LaNi$_4$Al sample compared to that determined for
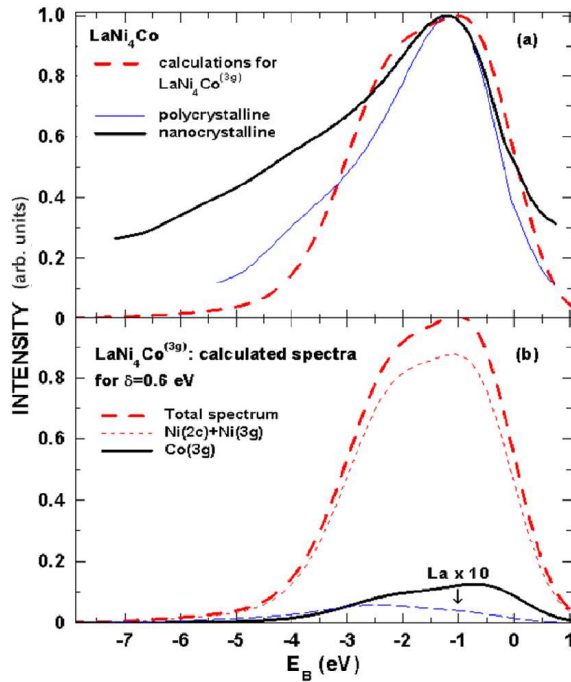
Fig. 3. Experimental (bold and thin solid line, top part) and theoretical (bold broken line, top part) XPS valence band spectra for *in situ* prepared nano- and polycrystalline LaNi$_4$Co alloy thin films. Local contributions of Ni, Co, and La atoms to the total theoretical XPS spectrum are shown in bottom part.

Fig. 4. Experimental (bold and thin solid line) and theoretical (bold broken line) XPS valence band spectra for *in situ* prepared nano- and polycrystalline LaNi$_4$Co alloy thin films (a). Local contributions of Ni, Co, and La atoms to the total theoretical XPS spectrum are also shown (b).

the polycrystalline thin film. Furthermore, the above results are in good agreement with theoretical XPS from *ab initio* band structure calculations. On the other hand, the XPS valence band of the bulk nanocrystalline LaNi$_{4.2}$Al$_{0.8}$ alloy reported in Ref. [4] is considerably broader and shifted compared to those measured for the thin film samples. The above behaviour was explained as strong deformation of the nanocrystals in mechanically alloyed and heat treated nanocrystalline samples. Such a modification of the valence band of the nanocrystalline LaNi$_{4.2}$Al$_{0.8}$ alloy compared to that measured for the polycrystalline sample could significantly improve the discharge capacity [4]. In Figs. 3 and 4 (bottom part) we have not shown theoretical XPS contribution from Al and Co atoms located in 2c positions due to considerable disagreement with experimental results. This is in accordance with neutron spectroscopy experiment [11] which revealed 3g position for Al and Co substitute atoms.

4. Conclusions

In general, we have observed a good agreement between calculated and measured spectra for the polycrystalline samples. On the other hand, the different microstructure of the nanocrystalline samples leads to a significant modification of their valence band spectra, especially for the LaNi$_4$Co thin film. Such a modification could significantly influence its hydrogenation properties.

Acknowledgments

References

[1] L. Schlapbach, *Nature (London)* **460**, 809 (2009).

[2] L. Schlapbach, in: *Hydrogen in Intermetallic Compounds II*, Springer, Berlin 1992, p. 165.

[3] R. Griessen, *Phys. Rev. B* **38**, 3690 (1988).

[4] L. Smardz, M. Nowak, M. Jurczyk, *Int. J. Hydrogen En.* **37**, 3659 (2012).

[5] A. Pundt, C. Sachs, M. Winter, M.T. Reetz, D. Fritsch, R. Kirchheim, *J. Alloys Comp.* **293-295**, 480 (1999).

[6] L. Smardz, U. Köbler, W. Zinn, *J. Appl. Phys.* **71**, 5199 (1992).

[7] K. Köpernik, H. Eschrig, *Phys. Rev. B* **59**, 1743 (1999).

[8] K. Köpernik, B. Velicky, R. Hayn, H. Eschrig, *Phys. Rev. B* **55**, 5717 (1997).

[9] J.J. Yeh, I. Lindau, *At. Data Nucl. Data Tables* **32**, 1 (1985).

[10] M.R. Fitzsimmons, J.A. Estman, R.A. Robinson, A.C. Lawson, J.D. Thompson, R. Morshovich, *Phys. Rev. B* **48**, 8245 (1993).

[11] J.-M. Joubert, R. Černy, M. Latroche, A. Percheron-Guégan, K. Yvon, *J. Appl. Crystallogr.* **31**, 327 (1998).